A Sustainable Energy Management System for Isolated Microgrids

Bharatkumar V. Solanki, *Student Member, IEEE*, Kankar Bhattacharya, *Fellow, IEEE*, and Claudio A. Cañizares, *Fellow, IEEE*

***Abstract*—In this paper, the equivalent CO_2 emission models for fossil-fuel-based distributed generator units are developed considering their individual emission characteristic and fuel consumption. These models are then integrated within a microgrid energy management system (EMS) model. Constant energy, demand shifting load models are further integrated in the EMS to examine the possible impact of demand response (DR) on the total system emissions and economics of a microgrid. Thus, the impacts of including the developed emission models on the operation of an isolated microgrid, equivalent CO_2 emissions, and costs are examined considering five different operating strategies. The proposed operating strategies are validated on a modified CIGRE medium voltage benchmark system. The results obtained highlight the effectiveness of the proposed EMS and also demonstrate the impact of DR on emissions and costs.**

***Index Terms*—Demand response, emission model, energy management systems, microgrids, sustainability.**

NOMENCLATURE

Indices, Sets and Superscripts

g	Distributed generator (DG) unit
G_i	Set of DG units connected to bus *i*
i, j	Bus
k	Time-step [min]
n	Energy Storage System (ESS) unit
N_i	Set of ESS units connected to bus *i*
p	Pollutant type (CO_2, CO and NO_x)
t	Time [min]
c	Commercial
r	Residential

Parameters

a	Quadratic term of cost function of DG unit [\$/(kWh)^2]
a^{em}	Quadratic term of emission function of DG unit [tonne/(kWh)^2]
A_1	Aspiration level for operating cost [\$]
A_2	Aspiration level for emission cost [\$]
b	Linear term of cost function of DG unit [\$/kWh]
b^{em}	Linear term of emission function of DG unit [tonne/kWh]
c	Constant term of cost function of DG unit [\$/h]
C^{em-sdn}	CO_2 emission associated with shut-down of DG unit [tonne]
C^{em-sup}	CO_2 emission associated with start-up of DG unit [tonne]
c^{em}	Constant term of emission function of DG unit [tonne/h]
C^{LC}	Load curtailment cost [\$/kWh]
C^{sup}, C^{sdn}	Start-up and shut-down cost of DG unit [\$]
PD	Active power demand [kW]
$\overline{PW}$	Wind turbine output [kW]
$\overline{PESS}$	Charging/discharging power limit of ESS unit [kW]
PV	Photo-Voltaic (PV) unit output [kW]
R^{sv}	Spinning reserve factor
R^{up}, R^{dn}	Ramp-up and ramp-down rate of DG unit [kW/h]
T^{up}, T^{dn}	Minimum-up and -down time of DG unit [h]
w	Weight applied to D_1 and D_2
α	Emission Factor for a pollutant of DG unit [tonne/MBTU]
β	Global Warming Potential Index
Δt	Absolute time between time steps [h]
η^{ch}, η^{dch}	Charging and discharging efficiency of ESS unit
γ	Social cost of CO_2 emissions [\$/tonne]
$\underline{\cdot}, \overline{\cdot}$	Minimum, maximum variable limits
$\tilde{\cdot}$	Normalized variable

Variables

D_1, D_2	Deviations from aspiration level for operating and equivalent CO_2 emission costs, respectively [\$]
E	Pollutant p emission from DG unit [tonne]
E^{CO_2}	Equivalent CO_2 emission of pollutant from DG unit [tonne]
J_{cp}	Normalized distance function
J_{em}	Equivalent CO_2 emission cost [\$]
J_{gp}	Weighted sum of D_1 and D_2 [\$]
J_{oc}	Sum of J_{op} and J_{em} [\$]
J_{op}	Operating cost [\$]
L	Fuel consumption of DG unit [MBTU]
P	Active power from DG unit [kW]
P^{ch}, P^{dch}	Charging and discharging power of ESS unit [kW]
P^{LC}	Load curtailed [kWh]

Manuscript received November 7, 2016; revised February 23, 2017; accepted March 30, 2017. Date of publication April 12, 2017; date of current version September 15, 2017. This work was supported by the NSERC Smart Microgrid Network (NSMG-NET), Canada. Paper no. TSTE-00863-2016. *(Corresponding author: Kankar Bhattacharya.)*

The authors are with the Department of Electrical and Computer Engineering, University of Waterloo, Waterloo, ON N2L3G1, Canada (e-mail: b2solanki@uwaterloo.ca; kankar@uwaterloo.ca; ccanizar@uwaterloo.ca).

Color versions of one or more of the figures in this paper are available online at http://ieeexplore.ieee.org.

Digital Object Identifier 10.1109/TSTE.2017.2692754

S	Shut-down decision of DG unit (1 = shut-down, 0 = otherwise)
SOC	State of charge of ESS unit
U	Start-up decision of DG unit (1 = start-up, 0 = otherwise)
W	ON/OFF decision of DG unit (1 = ON, 0 = OFF)

I. Introduction

INCREASING concerns on green house gas (GHG) emissions and continuous reductions in the cost of renewables based generation resources are encouraging the penetration of Distributed Energy Resources (DERs) and demand side management options in electrical systems [1]. For a successful integration of DERs, the concept of microgrids has evolved [2], [3], where microgrid is defined as a group of interconnected loads and DERs such as distributed generators (DG), energy storage systems (ESS), and controllable loads, within a clearly defined electrical boundary that can act as a single controllable entity with respect to the grid. Microgrids can be permanently connected to the grid, isolated from the grid, or can shift from one mode to the other. There are many remote communities worldwide which are not connected to the grid, and meet their electricity demand mainly from fossil fuel based DG units in isolated microgrids (e.g., [4]).

The Energy Management System (EMS) of microgrids determines the optimal dispatch and schedules of the DERs and are hence responsible for their economic and reliable operation [2], [3], [5]. These isolated microgrids rely on fossil-fuel-based DG units to meet the electricity demand, and are known to be high emitters of GHGs; for example, amongst the 280 remote communities in Canada, more than 50% of installed capacity are diesel-based DG units [4]. High level of diesel-based generation in isolated communities raises environmental and other socio-economic concerns. Therefore, there is a need to explore options other than energy supply from fossil fuels, through the use of renewable-based DG units to balance the demand and supply in these microgrids to reduce the impact on the environment [4]. Furthermore, Demand Response (DR) is another viable option for isolated microgrids for emissions and cost reductions, since is readily implementable and available, as well as environmentally friendly and cheaper than investments in generation resources [6].

Customer participation in energy management via DR programs by curtailing and/or shifting controllable demand has been shown be effective in distribution feeder operation [7], [8]. The positive impact of DR on the operation and costs of isolated microgrids has been analyzed in the literature [6], [9]–[11]. However, the impact of DG units and DR on equivalent CO_2 emissions in microgrids need to be quantified and better examined. Hence, this paper proposes DG CO_2-emission models for microgrid EMS formulations to study the impact of DG and DR in emissions and operating costs.

In [12], a Unit Commitment (UC) based microgrid EMS is proposed, which comprises a multi-objective function seeking simultaneous minimization of fuel consumption and pollutant emissions, and considers dispatchable and non-dispatchable DG units and ESS; the pollutant emissions from the DG units are considered to be nonlinear functions of the power output of the DG unit, based on the specific emission and a global warming potential of each pollutant. An Optimal Power Flow (OPF) based EMS with multi-objective function considering simultaneous minimization of operation cost, emission, and use of ESS is proposed in [13] for isolated microgrids. The pollutant emissions from DG units are modeled as linear functions of the power output of the DG unit. It is important to note that none of these works consider demand management schemes to account for customer participation in energy management.

As part of various demand side management (DSM) and DR schemes, customers can participate in energy management by shaving and/or shifting loads during the peak load hours or system contingencies which in turn increases the reliability of the system and benefits both customers and utilities [7], [8]. Thus in [7], a short-term power scheduling model, simultaneously considering the linearized power flow and UC constraints, is proposed for distribution systems with fossil-fuel-based DG units; the demand is considered to respond to real time pricing (RTP) and is expressed by price elasticity coefficients in the energy management problem; however, the proposed EMS considers only fossil-fuel-based generators nor renewable-based DG units. In [9], to analyze the impact of different DR options on an isolated microgrid operation, peak shaving and load shifting schemes are modeled using associated cost and price elasticity coefficients that are integrated in the EMS; the results indicate potential reductions in operation costs in the presence of DR since fewer thermal units are committed.

In [14], five different objectives including energy costs, non-delivered energy, power purchase/sell to the grid, peak loading, and emissions are considered along with their weighted sum to determine the optimal dispatch of the DERs in a grid-connected microgrid. The emissions from the DG unit are modeled as quadratic functions of the DG power output, considering fuel consumption and the corresponding pollutant emission; moreover, load curtailment is considered with associated costs of energy curtailment. Heuristic based UC models are presented in [15] and [16] for day-ahead operation of grid-connected microgrids. In [15], the operating and emission costs are minimized to obtain the optimal dispatch of DERs including ESS and electric vehicles as controllable demand, considering predetermined emission characteristic of the DG units from [17] and generation from renewable sources. In [16], the operating and emission costs are minimized in a grid-connected microgrid considering curtailable demand, vehicle-to-grid, and DG units, with their respective predetermined emission characteristics from [18]; ESS and generation from renewable sources are not considered. The formulated UC-based dispatch algorithms for grid-connected microgrids in [14]–[16] do not take into account start-up and shut-down operation costs and associated pollutant emissions, nor consider forecast deviation of renewables and demand.

Isolated microgrids have to manage their energy needs using available resources, and if the renewables based DG units contribute significantly to the dispatch, the deviation in the forecast of renewables can adversely affect the reliable operation of the microgrid. Thus, dispatch decisions must be made considering forecast deviations, which is frequently done by adopting certain control techniques such as a Model Predictive Control

(MPC) [19]. A UC with MPC is proposed in [6], [10], [19] for renewable-based microgrids. Furthermore, in [6], load shifting is included in the EMS to account for customer's participation, while load shaving is considered in the EMS proposed in [10]. In [11], an integrated UC and OPF EMS with an MPC approach is presented, considering controllable demand as a function of ambient temperature, time-of-use electricity price, demand limit, and time of the day. However, these papers do not take into account emissions from DG units in the EMS formulation.

There is no reported attempt to develop a detailed UC model for isolated microgrid with all DER related constraints that includes pollutant emission models, while accounting for deviations in the forecast of the renewable and DR schemes. Hence, this paper presents a mathematical model of such a comprehensive UC, which simultaneously minimizes operating costs and pollutant emissions considering demand-shifting load models. In addition, an MPC approach is used to consider the deviations in the forecast of renewables and electricity demand. Thus, the contributions of this work are as follows:

1) Equivalent CO_2 emission models of DG units are proposed, considering their individual emission characteristic and fuel consumption. These models are then integrated within the microgrid UC model.
2) Demand-shifting load models are integrated into the UC to examine the possible impact of DR on the total system emissions and costs.
3) A multi-objective UC model is developed to study the impact of microgrid operation on emissions and costs for different operating strategies, while considering the deviation in the forecast of renewables and demand through an MPC approach.

The rest of the paper is organized as follows: Section II presents the emission models, different objective functions, and the mathematical UC model and its implementation for microgrid dispatch. Section III presents the test system and case studies considered, and presents some of the more relevant results obtained with the proposed UC models, discussing their main features. Finally, Section IV highlights the main conclusions and contributions of this paper.

II. Mathematical Modeling

A. Emission Model of Generators

The emission models of fossil-fuel-based DG units are proposed here, representing the mathematical relationship between the loading level of DG units and the associated amount of pollutant emissions, namely, carbon dioxide (CO_2), nitrogen oxide (NO_x) and carbon monoxide (CO). The emissions at different loading levels of DG units can be obtained as follows:

$$E_{p,g}(P_g) = \alpha_{p,g}(P_g) L_g(P_g) \qquad \forall p, g \tag{1}$$

where all variables and parameters in this and other equations are defined in the Nomenclature section. The amount of pollutant emissions per unit fuel combustion $\alpha_{p,g}$ can be found in [20].

The equivalent CO_2 emission from each pollutant can be determined by multiplying the Global Warming Potential Index (GWPI), of the pollutant β_p, given in [21], with the respective pollutant emissions, as follows:

$$E^{\mathrm{CO_2}}_{p,g}(P_g) = \beta_p E_{p,g}(P_g) \qquad \forall p, g \tag{2}$$

The equivalent CO_2 emission from a DG unit can then be determined by summing the equivalent CO_2 emissions of each pollutant as follows:

$$E^{\mathrm{CO_2}}_{g}(P_g) = \sum_{p} E^{\mathrm{CO_2}}_{p,g}(P_g) \qquad \forall g \tag{3}$$

Therefore, $E^{\mathrm{CO_2}}_{g}(P_g)$ can be expressed using (1) and (2) as follows:

$$E^{\mathrm{CO_2}}_{g}(P_g) = \sum_{p} \beta_p \alpha_{p,g}(P_g) L_g(P_g) \qquad \forall g \tag{4}$$

where it can be observed that the emission from a DG unit is directly dependent on its loading level.

The equivalent CO_2 emission from a DG unit operating at a given loading level at time t can also be expressed in general form as follows [12]:

$$E^{\mathrm{CO_2}}_{g,k}(P_{g,k}) = \left(a^{em}_g P^2_{g,k} \Delta t_k + b^{em}_g P_{g,k} + c^{em}_g W_{g,k}\right) \Delta t_k + C^{em-sup}_g U_{g,k} + C^{em-sdn}_g S_{g,k} \quad \forall g, k \tag{5}$$

which is a generic quadratic function depicting the relationship of equivalent CO_2 emissions with the DG loading level. Note also that (5) includes equivalent CO_2 emissions associated with DG unit start-up and shut-down, where the start-up emission coefficient C^{em-sup}_g denotes the amount of CO_2 emission during the DG unit start-up, which is assumed equivalent to 5 min of full load operation of the DG unit, while the shut-down coefficient C^{em-sdn}_g denotes the CO_2 emission during shut-down operation, which is assumed equivalent to 2.5 min full load operation of the DG unit [12]. From (4) and (5), the coefficients a^{em}_g, b^{em}_g, and c^{em}_g can be determined using a simple curve-fitting technique. Hence, the mathematical model for CO_2 emission from a DG unit given by (5) can be integrated into the microgrid UC model as discussed next.

B. Microgrid UC Model

The model is developed from the perspective of the operator, who seeks to minimize the operating costs of the microgrid, including generation costs, and start-up and shut-down costs. Such objective can be expressed as follows,

$$J_{op} = \sum_{g,k} \left[(a_g P^2_{g,k} \Delta t_k + b_g P_{g,k} + c_g W_{g,k}) \Delta t_k + C^{sup}_g U_{g,k} + C^{sdn}_g S_{g,k}\right] \tag{6}$$

In addition, the following constraints can be defined to represent the operational constraints of the microgrid:

1) *Demand Supply Balance:* These constraints ensure that total the generation meets the total demand of the microgrid

at each time step:

$$\sum_g P_{g,k}W_{g,k}+\sum_i (PV_{i,k}+PW_{i,k})+\sum_n (P^{dch}_{n,k}-P^{ch}_{n,k}) = \sum_i \left[PD^c_{i,k}+PD^r_{i,k}+PD^{rs}_k\right] \quad \forall k \tag{7}$$

It is assumed that a part of the residential load PD^{rs}_k is controllable and hence is an optimization variable, as it can be shifted to other hours. The rest of the load, which is uncontrollable, can be obtained using a forecasting engine.

2) *Reserve Constraints:* These constraints ensure that the spinning reserve requirement is met by the dispatched generators, as follows:

$$\sum_g (\bar{P}_g - P_{g,k})W_{g,k} \geq R^{sv}\sum_i \left[PD^c_{i,k}+PD^r_{i,k} + PD^{rs}_k + PV_{i,k}+PW_{i,k}\right] \quad \forall k \tag{8}$$

3) *DR Constraints:* The controllable demand PD^{rs}_k is a power-shifting demand that can be shifted and at least paid back within the same day, considering the maximum and minimum limits of the shiftable demand. This can be modeled as follows:

$$\sum_k PD^{rs}_{i,k}\Delta t_k \geq 0 \quad \forall i \tag{9}$$

$$\underline{PD}^{rs}_i \leq PD^{rs}_{i,k} \leq \overline{PD}^{rs}_i \quad \forall i,k \tag{10}$$

4) *UC Constraints:* These constraints include active and reactive power generation limits, ramp-up and ramp-down constraints, minimum up-time and down-time constraints, and coordination constraints, as discussed in detail in [11].

5) *Energy Storage System:* The ESS model comprises the energy balance equation, a constraint to restrict simultaneous charging and discharging, and a constraint to limit the SOC and charging-discharging power, as discussed in detail in [11].

C. Operating Strategies

The next five different operating strategies are considered to study the optimal dispatch of microgrid DG units and the role of DR in system emissions and costs.

1) Operating Cost Minimization (Case 1 or Base Case): The operating costs of the microgrid includes generation cost, start up and shut down costs as given in (6). This case represents the current EMS practice in isolated microgrids, and is not sustainable from a long-term perspective. The next four cases include the proposed emission models, thus representing sustainable models.

2) Emission Cost Minimization (Case 2): The equivalent CO_2 emission cost for fossil-fuel based DG units is obtained by multiplying the social cost of equivalent CO_2 emissions γ with the total equivalent CO_2 emissions from generation, start-up and shut-down operations, as per (5), and is given by:

$$J_{em} = \gamma \sum_{g,k} \left[(a^{em}_g P^2_{g,k}\Delta t_k + b^{em}_g P_{g,k} + c^{em}_g W_{g,k})\Delta t_k + C^{em-sup}_g U_{g,k} + C^{em-sdn}_g S_{g,k}\right] \tag{11}$$

3) Minimization of Emission and Operating Costs (Case 3): In order to consider the pollutant emissions and the operating cost of DG units simultaneously in the formulation of the EMS objective function, one of the strategies is to minimize the algebraic sum of equivalent CO_2 emission costs and operating costs. The key feature of this multi-objective strategy is that it does not require prior knowledge of the aspiration levels of these conflicting objectives, their minimum or maximum values, nor the weights associated with them to obtain an optimal dispatch. Such an objective function can be expressed as follows:

$$J_{oc} = J_{op} + J_{em} \tag{12}$$

4) Pareto-Optimality of Operating and Emission Costs (Case 4): In this case, the objective function is formulated considering both the operating costs and emission costs as a normalized function to obtain the Pareto-optimal solution between the two objectives, as follows:

$$J_{cp} = \sqrt{\left(\frac{J_{op}-\underline{J}_{op}}{\bar{J}_{op}-\underline{J}_{op}}\right)^2 + \left(\frac{J_{em}-\underline{J}_{em}}{\bar{J}_{em}-\underline{J}_{em}}\right)^2} \tag{13}$$

5) Minimization of Deviation of Operating and Emission Costs (Case 5): In this case, the objective function seeks to minimize the weighted sum of two quantities: the deviations in the operating costs from its aspiration level, and the deviation in the equivalent CO_2 emission costs from its aspiration level, as follows:

$$J_{gp} = wD_1 + (1-w)D_2 \tag{14}$$

where

$$D_1 = J_{op} - A_1 \tag{15}$$

$$D_2 = J_{em} - A_2 \tag{16}$$

and A_1 and A_2 are the aspiration levels of operating and emission costs, respectively. The aspiration levels are the desired target values of the objective function such as operating cost or emissions, which are set by the system operator, planner, or policy maker. In the present work, the aspiration level of the operating cost A_1 is considered to be the minimum operating cost obtained from Case 1, while the aspiration level of emission cost A_2 is set at the minimum emission cost obtained from Case 2. These are stiff targets to achieve simultaneously, and represents the "ideal" solution, which the model "aspires" to attain.

D. Scheduling Time Horizons and MPC

The forecasts of demand and generation from renewables are more accurate for a shorter look-ahead window, with the forecast errors increasing as the look-ahead window is broadened [11], [19]. Furthermore, since a uniform 5 min time resolution over a 24-hour look-ahead window requires large computational resources to solve the UC problem, a scheduling horizon with

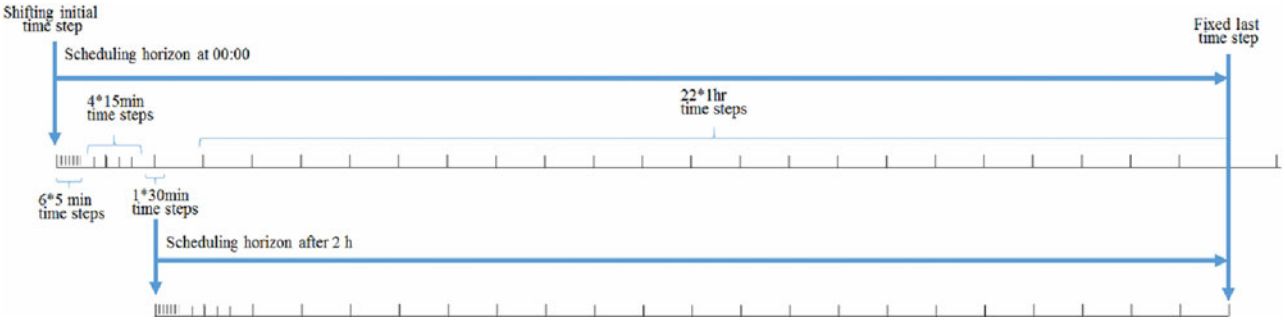

Fig. 1. Scheduling time horizon.

non-uniform time resolution is used, with short few times steps first and increasing time steps after, as discussed in [11], [19]. The considered scheduling horizon is shown in Fig. 1.

In isolated microgrids, the generation from renewables contribute a significant share to the energy supply mix. Hence, the optimal dispatch of the controllable DERs rely on the forecast of generation from renewables, which varies over the time horizon. Thus, an MPC approach is adopted here, where the dispatch problem is re-solved considering updated forecast of the generation from renewables at every 5 minute re-calculation time interval, as explained in [11], [19]. The obtained UC dispatch of DERs is valid only for the next time interval. Moreover, in order to balance the shiftable demand over a day and also to maintain the SOC level at the end of the day, the time horizon is considered to be receding at every re-calculation iteration, in which the initial time step is shifted forward by one time interval, while the last time step is kept fixed, as depicted in Fig. 1.

III. Results and Discussions

The proposed operating strategies for the proposed EMS model are tested here on the CIGRE medium voltage benchmark network depicted in Fig. 2 [19], which has been modified to consider 25% more ESS capacity, and a total installed capacity of 9,216 kW from all DG units [11]. The DER costs are extracted from [19], and the social cost of equivalent CO_2 emissions γ is assumed to be 37 \$/tonne [22].

As discussed in Section II-A, based on the emission data sheet of the respective generators and their emission factors [20], [23], the obtained equivalent CO_2 emission characteristics of the five DG units are shown in Fig. 3, and the corresponding co-efficients of the equivalent CO_2 emission functions are shown in Table I. Note from Fig. 3 that DG unit G13 accounts for the highest equivalent CO_2 emission in tonne/kWh, and its emission level is significantly higher compared to the other DG units; units G3, G1, G9 and G2 follow suit in decreasing order of emissions.

As discussed in Section II-C, five distinct operating strategies (UC objective functions) are considered to examine the microgrid EMS model performance. In order to study the impact of DR on pollutant emissions, all these cases are also discussed here without considering DR by forcing $PD^{rc}_{i,k} = 0, \forall i, k$.

All the models were coded and solved in GAMS [24], on an Intel(R) Xeon(R) CPU L7555, 1.87 GHz 4-processor server. In Cases 1, 2, 3 and 5, the objective functions are quadratic

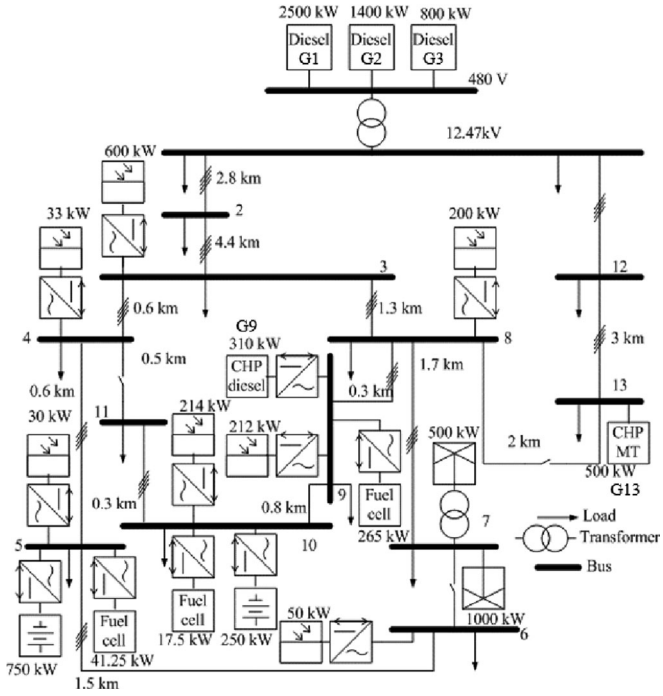

Fig. 2. Modified CIGRE microgrid benchmark [11], [19].

functions, and hence these are Mixed Integer Quadratic Programming (MIQP) problems, which can be solved using the CPLEX solver [25]. On the other hand, Case 4 has a non-linear objective function, and hence is a Mixed Integer Non-Linear Programming (MINLP) problem, which can be solved using the DICOPT solver [25]. All case studies, with and without DR, were simulated for 24 hours of system operation using the MPC approach, with a re-calculation time of 5 minutes. A warm start was used in the solution process, in which a previously obtained feasible solution was applied as the starting point for the next solution. In case of in-feasibility in the solution process, the optimization model was re-solved by initializing the binary decision variables to the ON state [11].

The wind and solar PV profiles shown in Fig. 4 were used here, based on actual measured data from wind and solar plants in the Kasabonika Lake First Nation community microgrid [26]. The demand profiles were the same as those used in [19]. Normal probability density functions of day-ahead and 1-hour ahead forecasting errors were used to simulate wind, solar and demand

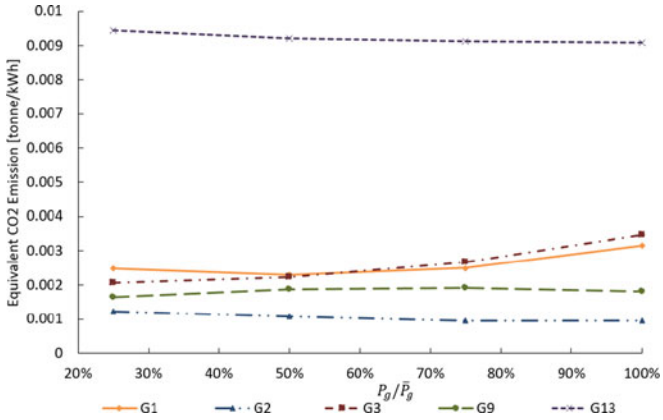

Fig. 3. Emission characteristics of DG units.

TABLE I
PARAMETERS OF THE DG EMISSION CHARACTERISTICS

DG units	G1	G2	G3	G9	G13
$\bar{P}_g$, MW	2.5	1.4	0.8	0.31	0.5
a_g^{em}	1.2228	0.0234	4.3792	0	0.0088
b_g^{em}	−0.48236	0.8114	−0.4755	1.8849	8.9722
c_g^{em}	1.4235	0.1505	0.3449	−0.0087	0.0594
C_g^{em-sup}	0.0712	0.1075	0.0165	0.0479	0.3788
C_g^{em-sdn}	0.0356	0.0537	0.0082	0.0239	0.1894

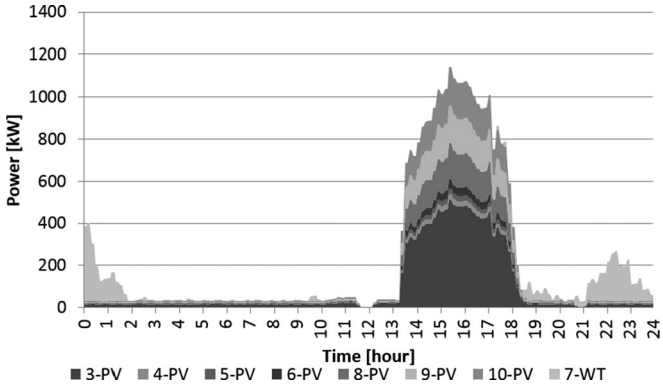

Fig. 4. Solar PV and wind generation profiles.

power forecasts in the EMS model. Every 5 minutes, renewable generation and load forecasts were computed based on a linear approximation of the difference between the 24-hour and 1-hour ahead forecast errors, with respect to time. This approach to generate renewables and demand forecast is discussed in more detail in [11].

Table II presents the EMS results obtained without and with DR, including the total equivalent CO_2 emissions in each case and its % reduction with respect to Case 1. Figs. 5 and 6 presents plots of normalized operating costs $\widetilde{J}_{op}$ versus normalized emission costs $\widetilde{J}_{em}$ for all the cases without and with DR, respectively, where these normalized costs are defined as

TABLE II
SUMMARY OF MICROGRID EMS OPERATING STRATEGIES

	Cases	1	2	3	4	5
Without DR	J_{op} [$]	15,198	18,996	17,547	16,730	16,707
	J_{em} [$]	10,351	5,422	6,538	7,869	7,276
	Emissions [Tonne]	279.8	146.6	176.7	212.7	199.6
	Reduction in emissions [%]	0	48	37	24	29
	Increase in op. costs [%]	0	25	15	10	10
	Average CPU time per MPC iteration [s]	6.67	22.7	36.25	8.12	5
With DR	J_{op} [$]	14,971	18,906	17,862	16,394	16,491
	J_{em} [$]	10,593	5,103	5,982	7,865	7,443
	Emissions [Tonne]	286.3	137.9	161.7	212.6	201.2
	Reduction in emissions [%]	0	52	44	26	30
	Increase in op. costs [%]	0	26	19	9.5	10
	Average CPU time per MPC iteration [s]	13.75	43.12	47.08	8.12	17.29

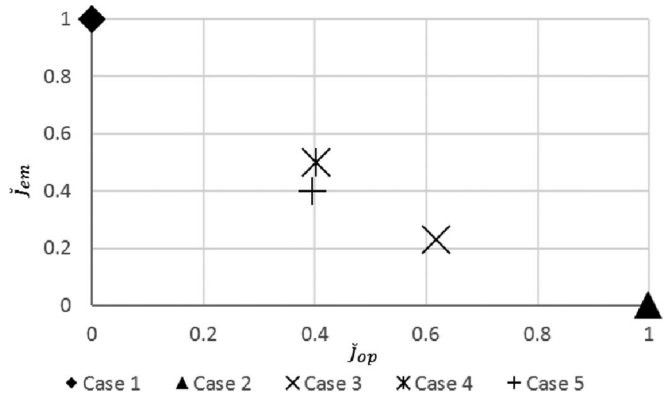

Fig. 5. Normalized operating costs vs. normalized emission costs without DR.

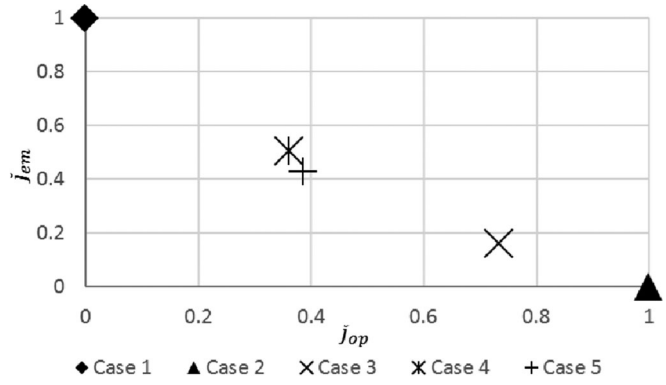

Fig. 6. Normalized operating costs vs. normalized emission costs with DR.

follows:

$$\widetilde{J}_{op} = \frac{J_{op} - \underline{J}_{op}}{\bar{J}_{op} - \underline{J}_{op}} \tag{17}$$

$$\widetilde{J}_{em} = \frac{J_{em} - \underline{J}_{em}}{\bar{J}_{em} - \underline{J}_{em}} \tag{18}$$

Figs. 7 and 8 present the share of individual DG units in the microgrid EMS dispatch without and with DR, respectively.

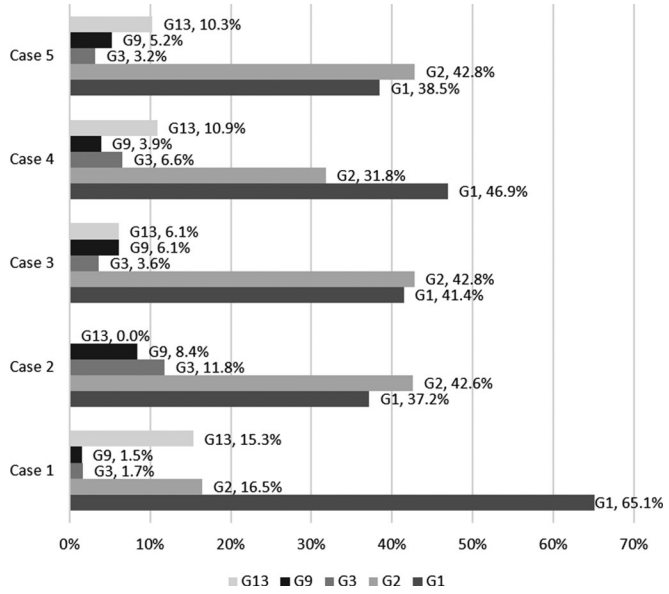

Fig. 7. Dispatch contribution of DG units without DR.

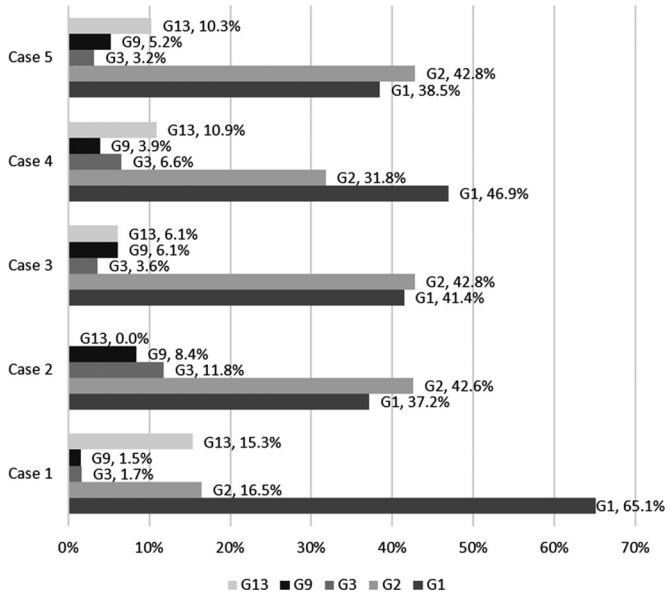

Fig. 8. Dispatch contribution of DG units with DR.

Finally, Figs. 9–13 depict stacked area plots of the equivalent CO_2 profiles for each DG unit, for all cases, without and with DR. The following observations can be made for Table II and Figs. 5–13:

1) Case 1 yields the least operating cost dispatch but incurs the highest emission cost, which is to be expected, since in this case emissions are not considered. On the other hand, and as expected, Case 2 yields the least emission cost dispatch with the highest operating cost, both with and without DR. These cases account for the two extreme points in Figs. 5 and 6.
2) In Case 1 with DR, observe that operating costs are reduced by 1.5%, while emission costs increase by 2.3% (Table II) with respect to Case 1 without DR. This is because the shiftable demand is dispatched at off-peak hours so that the dispatch share of the cheapest unit G1 is increased while the dispatch from G2, which has least emissions (Fig. 3), is reduced (Figs. 7 and 8). The major changes in emissions with DR for Case 1 are highlighted in Fig. 9, where the emissions during off-peak hours (hours 0 to 6) and also during on-peak hours (hours 18 to 20) are increased, while a reduction in emissions is observed between hours 7 to 10.
3) In Case 2 with inclusion of DR, the emission and operating costs are reduced by 5.8% and 0.5% respectively (Table II) with respect to Case 2 without DR. The reason for this significant reduction is that the dispatch share of low emission units G2, G1, and G9 are increased, whereas unit G13, which has the highest emission (Fig. 3), is not committed, as the controllable demand is shifted to off-peak hours (Figs. 7 and 8). These observations can also be made in Fig. 10, during the highlighted off-peak hours, which shows reduction in emissions from G3 due to a reduced dispatch of this unit at these hours due to DR.
4) In Case 3, note that the introduction of DR reduces the sum of operating and emission costs, as compared to the case without DR, with the operating costs increasing by 1.8%, while the emission costs decrease by 8.5% (Table II). This can be attributed to the reduction in dispatch of G13, which has the highest emissions and the least operating costs, when DR is introduced. This is also depicted and highlighted for hours 18 to 21 in Fig. 11.
5) Case 4 yields a dispatch to minimize deviations from the optimal operating and emission costs. Observe in Figs. 5 and 6 that normalized operating costs are 0.4 and 0.36, and normalized emission costs are 0.49 and 0.5, without and with DR, respectively. Note in Table II that with DR, both operating and emission costs are reduced by 2% and 0.1% with respect to Case 4 without DR, respectively, because the dispatch share of G1 and G9 is increased, since G1 is the cheapest unit while G9 is a low-emission unit (Figs. 7 and 8). On the other hand, the dispatch share of unit G3, which has high emissions (Fig. 3), is reduced in coordination with the shifting of the controllable demand (Figs. 7 and 8). The reduction in emissions due to less use of G3 is also highlighted in Fig. 12. The reason for the higher reduction in operating cost as compared to the emission cost is that, in the objective function, $\frac{1}{J_{op}-\underline{J}_{op}}$ is larger than $\frac{1}{J_{em}-\underline{J}_{em}}$, which are the multiplication factors for each cost component in (13).
6) In Case 5, the best combination of weights for least operating and emission cost is obtained by running the microgrid EMS model with different values of w. The variations of normalized operating and emission costs with respect to w are depicted in Figs. 14 and 15, where the curves intersect at $w = 0.54$ and $w = 0.535$. With

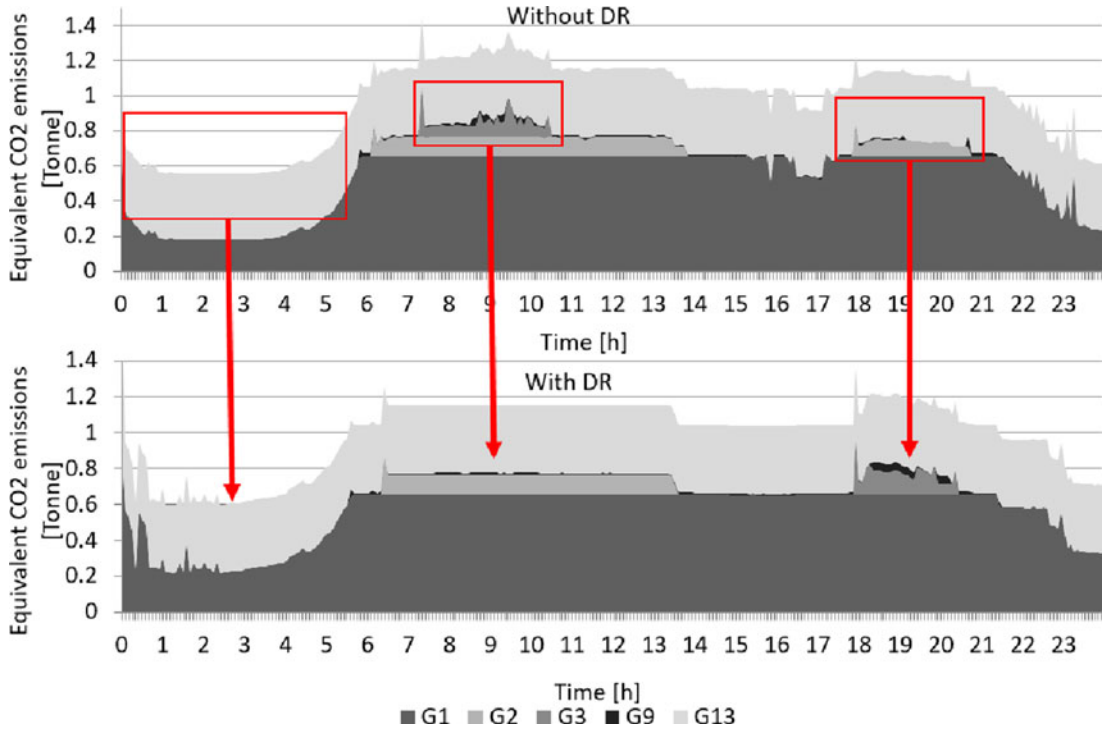

Fig. 9. Case 1 emission profiles of DG units without and with DR.

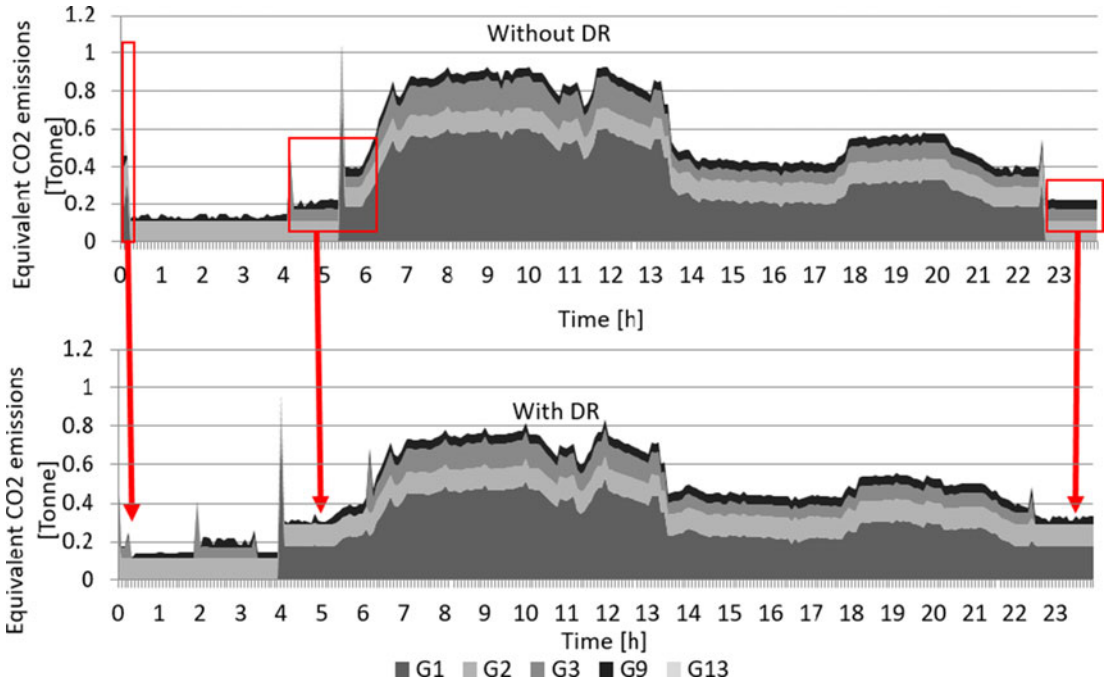

Fig. 10. Case 2 emission profiles of DG units without and with DR.

these values, observe Figs. 5 and 6 that the normalized operating and emission costs are closest to that obtained in Case 4, for both without and with DR. Note also that with DR for $w = 0.535$, the operating cost is reduced by 1.2% while emission cost is increased by 0.8% with respect to the case without DR (Table II), due to the increase in dispatch share of unit G13, which has the highest emission but least operating cost (Fig. 8). The increase in emissions with DR due to dispatch of G13 is also observed in Fig. 13.

7) It is important to note from Table II that with the consideration of the equivalent CO_2 emission model, the total equivalent CO_2 emissions are reduced from 24% to 48% without DR and from 26% to 52% with DR compared to Case 1, which does not include the emission function of

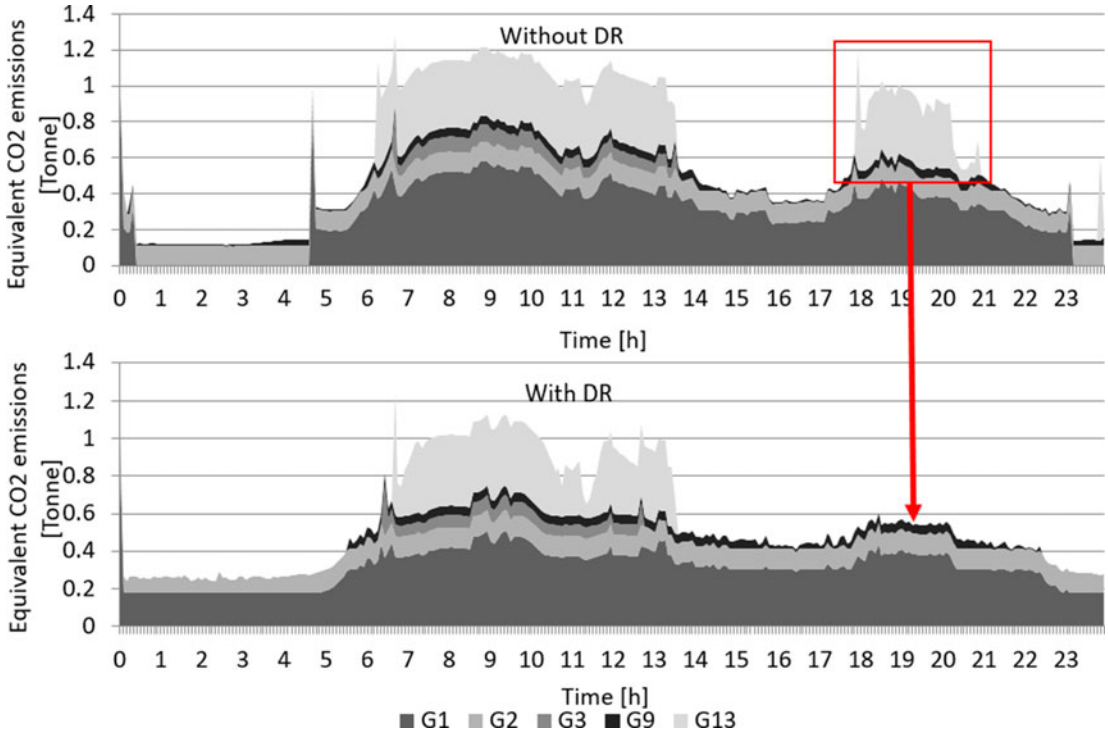

Fig. 11. Case 3 emission profiles of DG units without and with DR.

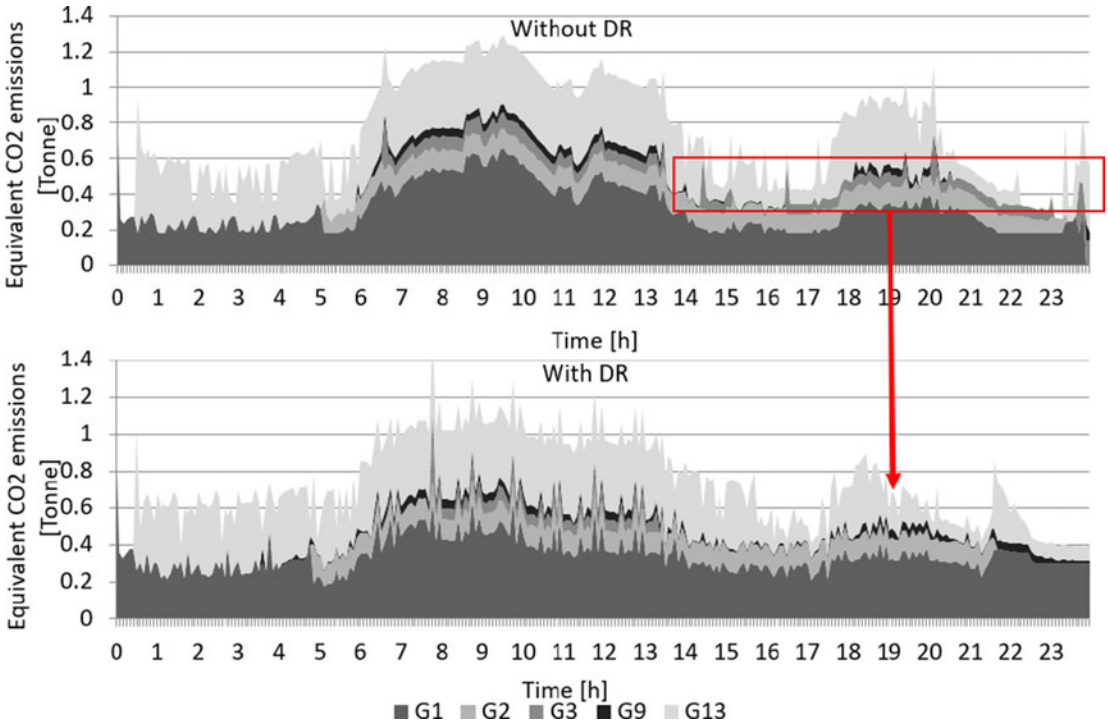

Fig. 12. Case 4 emission profiles of DG units without and with DR.

DG unit, demonstrating the environmental benefits of the proposed EMS models. However, there is an increase in operating cost in Cases 2 to 5, from 10% to 25% without DR, and 9.5% to 26% with DR, compared to the operating costs in Case 1, reflecting the impact of emission reductions in operating costs in the test system. Observe that among all operating strategies, Case 4 provides the dispatch with least increase in operating cost with significant reduction in emissions compared to Case 1, also showings the positive impact on both cases of DR.

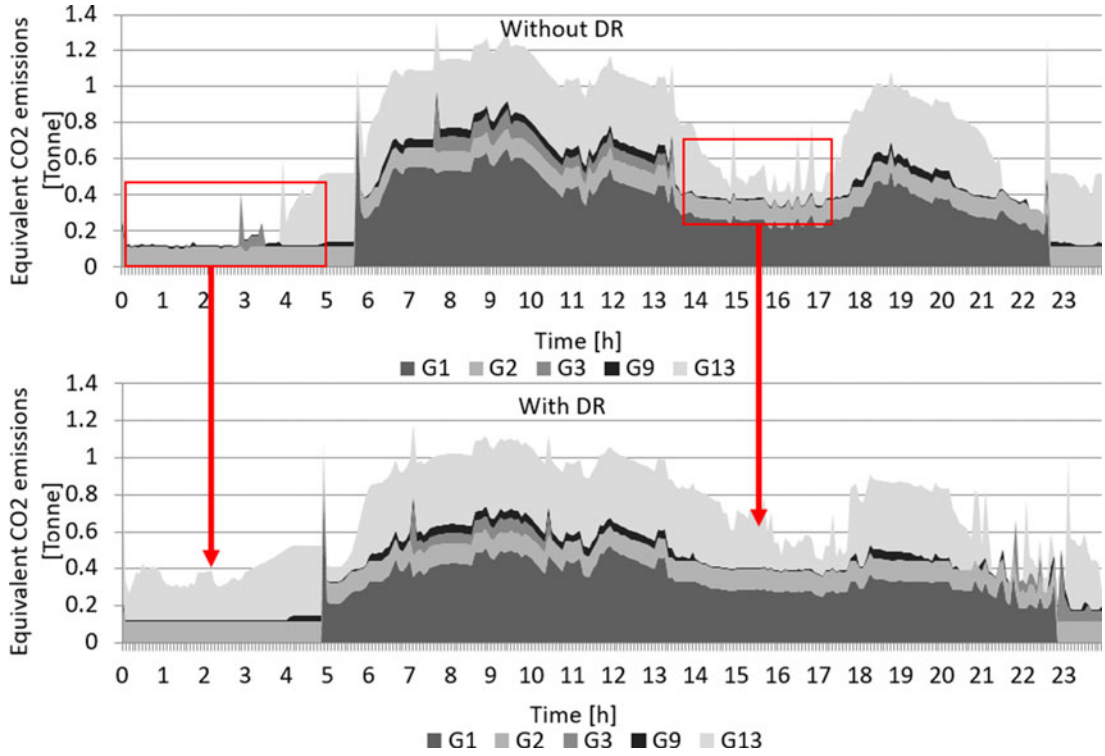

Fig. 13. Case 5 emission profiles of DG units without and with DR.

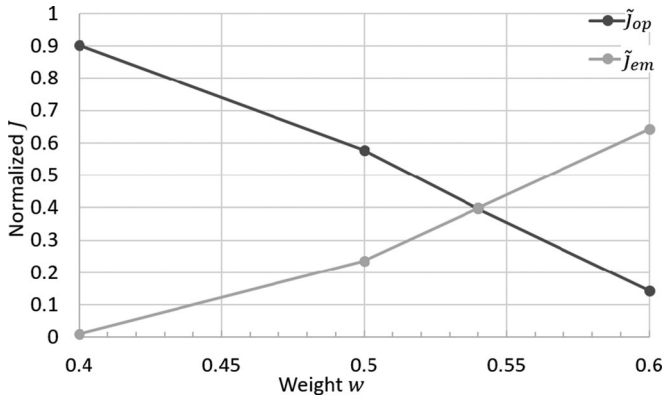

Fig. 14. Variation of J with weight w without DR.

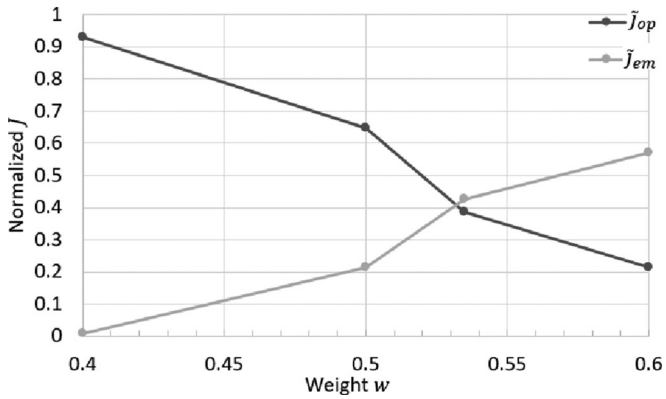

Fig. 15. Variation of J with weight w with DR.

8) The average computation (CPU) times per iteration of the MPC algorithm to obtain the 24 hour UC dispatch for all the cases, with and without DR, are shown in Table II. Observe that the CPU time increases in most of the cases when DR is included; however, the average computation time per MPC iteration is less than the required 5 min re-calculation time, and hence the proposed approach can be implemented in practical applications.

IV. Conclusion

In this paper, equivalent CO_2 emission functions were developed for DG units based on their emission factors and the GWPI of pollutants, and these equivalent CO_2 emission models were included in a microgrid EMS formulation; demand shifting loads were also included in the EMS model. To study the impact of equivalent CO_2 emission and operating costs simultaneously in microgrid dispatch, different operating strategies were developed, validated, and tested on a CIGRE microgrid benchmark system by using an MPC approach, considering the deviations in the forecast of demand and renewable generation.

The obtained results demonstrate that, with inclusion of DR, equivalent CO_2 emissions depend on the operating strategy, as the impact of DR on operating costs and equivalent CO_2 emission costs is different. From the presented studies, it can be concluded that the operating strategy that corresponds to Pareto-optimality of operating and emission costs provides the best possible compromise between the operating and equivalent CO_2 emission costs, reducing both costs with inclusion of DR. The operating strategy which minimizes the sum of both costs indeed

yields the least total costs; however, inclusion of both costs in the objective function does not guarantee reduction of these costs with DR. On the other hand, the operating strategy which minimizes the deviations in the aspiration levels of the two costs, with best possible weights, yields the dispatch solution closest to the Pareto-optimal solution.

REFERENCES

[1] S. Abolhosseini, A. Heshmati, and J. Altmann, "A review of renewable energy supply and energy efficiency technologies," IZA Institute of Labor Economics, Bonn, Germany, Tech. Rep. IZA DP No. 8145, Apr. 2014. [Online]. Available: http://ftp.iza.org/dp8145.pdf

[2] R. Lasseter, "Microgrid," in *Proc. IEEE Power Eng. Soc. Winter Meet.*, vol. 1, Jan. 2002, pp. 305–308.

[3] F. Katiraei, R. Iravani, N. Hatziargyriou, and A. Dimeas, "Microgrids management: Controls and operation aspects of microgrids," *IEEE Power Energy Mag.*, vol. 6, no. 3, pp. 54–65, May/Jun. 2008.

[4] M. Arriaga, C. A. Cañizares, and M. Kazerani, "Northen lights: Access to electricty in Canada's northern and remote communities," *IEEE Power Energy Mag.*, vol. 12, no. 4, pp. 50–59, Jul./Aug. 2014.

[5] D. E. Olivares *et al.*, "Trends in microgrid control," *IEEE Trans. Smart Grid*, vol. 5, no. 4, pp. 1905–1919, Jul. 2014.

[6] R. Palma-Behnke *et al.*, "A microgrid energy management system based on the rolling horizon strategy," *IEEE Trans. Smart Grid*, vol. 4, no. 2, pp. 996–1006, Jun. 2013.

[7] A. Safdarian, M. Fotuhi-Firuzabad, and M. Lehtonen, "Integration of price-based demand response in discos short-term decision model," *IEEE Trans. Smart Grid*, vol. 5, no. 5, pp. 2235–2245, Sep. 2014.

[8] I. Sharma, K. Bhattacharya, and C. Cañizares, "Smart distribution system operations with price-responsive and controllable loads," *IEEE Trans. Smart Grid*, vol. 6, no. 6, pp. 795–807, Mar. 2015.

[9] K. Dietrich, J. M. Latorre, L. Olmos, and A. Ramos, "Demand response in an isolated system with high wind integration," *IEEE Trans. Smart Grid*, vol. 27, no. 1, pp. 20–29, Feb. 2012.

[10] A. Parisio, E. Rikos, and L. Glielmo, "A model predictive control approach to microgrid operation optimization," *IEEE Trans. Control Syst. Technol.*, vol. 22, no. 5, pp. 1813–1827, Sep. 2014.

[11] B. V. Solanki, A. Raghurajan, K. Bhattacharya, and C. A. Cañizares, "Including smart loads for optimal demand response in integrated energy management systems for isolated microgrids," *IEEE Trans. Smart Grid*, to be published.

[12] H. Kanchev, F. Colas, C. Lazarov, and B. Francois, "Emission reduction and economical optimization of an urban microgrid operation including dispatched PV-based active generators," *IEEE Trans. Sustain. Energy*, vol. 5, no. 4, pp. 1397–1405, Oct. 2014.

[13] S. Conti, R. Nicolosi, S. A. Rizzo, and H. H. Zeineldin, "Optimal dispatching of distributed generators and storage systems for MV islanded microgrids," *IEEE Trans. Power Del.*, vol. 27, no. 3, pp. 1243–1251, May 2012.

[14] M. Ross, C. Abey, F. Bouffard, and G. Joós, "Multiobjective optimization dispatch for microgrids with a high penetration of renewable generation," *IEEE Trans. Sustain. Energy*, vol. 6, no. 4, pp. 1306–1314, Oct. 2015.

[15] C. Deckmyn, J. V. de Vyver, T. L. Vandoorn, B. Meersman, J. Desmet, and L. Vandevelde, "Day-ahead unit commitment model for microgrids," *IET Gener. Transmiss.. Distrib.*, vol. 11, no. 1, pp. 1–9, Jan. 2017.

[16] N. Zhang, Z. Hu, D. Dai, S. Dang, M. Yao, and Y. Zhou, "Unit commitment model in smart grid environment considering carbon emissions trading," *IEEE Trans. Smart Grid*, vol. 7, no. 1, pp. 420–427, Jan. 2016.

[17] B. Marti, "Emissions of power delivery systems," M.S. thesis, , Swiss Federal Inst. Technol. (ETH), Zurich, Switzerland, 2005.

[18] I. J. Raglend and N. P. Padhy, "Solutions to practical unit commitment problems with operational, power flow and environmental constraints," in *Proc. IEEE Power Eng. Soc. Gen. Meet.*, Jun. 2006, pp. 1–8.

[19] D. E. Olivares, C. A. Cañizares, and M. Kazerani, "A centralized energy management system for isolated microgrids," *IEEE Trans. Smart Grid*, vol. 5, no. 4, pp. 1864–1875, Jul. 2014.

[20] U.S. Environmental Protection Agency, "Compilation of air pollutant emission factor," U.S. Environmental Protection Agency, Washington, DC, USA, Tech. Rep. AP-42, Jan. 1995. [Online]. Available: https://www3.epa.gov/ttn/chief/ap42/index.html

[21] IPCC, "Climate change 2007: The physical science basis," Intergovernmental Panel on Climate Change, Geneva, Switzerland, Tech. Rep., 2007.

[22] U. S. Environmental Protection Agency , "Social cost of carbon," , U.S. Environmental Protection Agency, Washington, DC, USA, Tech. Rep., Dec. 2015. [Online]. Available: https://www3.epa.gov/climatechange/Downloads/EPAactivities/social-cost-carbon.pdf

[23] Cummins Power Generation, "Exhaust emission data sheet 2500DQLE," Cummins Power Generation, Ramsgate, U.K., Tech. Rep. eds-1116c, [Online]. Available: https://powersuite.cummins.com

[24] R. E. Rosenthal, "GAMS—A user's guide," GAMS Development Corporation, Washington, DC, USA, Tech. Rep., May 2015. [Online]. Available: http://www.gams.com/help/topic/gams.doc/userguides/GAMSUsersGuide.pdf

[25] GAMS, "GAMS – The solver manuals," , GAMS Development Corporation, Washington, DC, USA, Tech. Rep., May 2015. [Online]. Available: https://www.gams.com/latest/docs/solvers/allsolvers.pdf

[26] M. Arriaga, A. Madhavan, X. Wu, C. A. Cañizares, and M. Kazerani, "Database of electrical grid and microgrid systems in Canada's northern and remote communities," Hatch Ltd. Contract, ecoII NRCan project, Dep. Elect. Comput. Eng., Univ. of Waterloo, Waterloo, ON, Canada, Tech. Rep., Mar. 2014.

Bharatkumar V. Solanki (S'14) received the Bachelor's degree in electrical engineering from Gujarat University, Ahmedabad, India, in 2009, and the Master's degree in electrical engineering from the Maharaja Sayajirao University of Baroda, Vadodara, India, in 2011. He is currently working toward the Ph.D. degree in electrical and computer engineering at the University of Waterloo, Waterloo, ON, Canada. From 2011 to 2013, he was an Analog Hardware Design Engineer in ABB Global Industries and Service Limited, India. His research interests include modeling, simulation, control and optimization of power systems.

Kankar Bhattacharya (M'95–SM'01–F'17) received the Ph.D. degree in electrical engineering from the Indian Institute of Technology, New Delhi, India, in 1993. From 1993 to 1998, he was in the Faculty of Indira Gandhi Institute of Development Research, Mumbai, India, and in the Department of Electric Power Engineering, Chalmers University of Technology, Gothenburg, Sweden, from 1998 to 2002. In 2003, he joined the Electrical and Computer Engineering Department, University of Waterloo, Waterloo, ON, Canada, where he is currently a Full Professor. His research interests include power system economics and operational aspects. He is a Registered Professional Engineer in the Province of Ontario.

Claudio A. Cañizares (S'85–M'91–SM'00–F'07) received a Diploma degree from the Escuela Politecnica Nacional, Quito, Ecuador, and the M.S. and Ph.D. degrees from the University of Wisconsin Madison, Madison, WI, USA, in 1984, 1988, and 1991, respectively, all in electrical engineering. Since 1993, he has held various academic and administrative positions at the University of Waterloo, ON, Canada, where he is currently a Professor in the Department of Electrical and Computer Engineering and the Hydro One Endowed Chair. His research interests include stability, operating, control, modeling, simulation, and computational issues in sustainable power and energy systems in the context of competitive markets, smart grids, and microgrids. He was awarded the IEEE Canada Electric Power Medal in 2016, has received several IEEE Power and Energy Society (PES) Technical Committee and Council awards, and has held several leadership positions in PES Technical Committees and Subcommittees. He is a Fellow of the Royal Society of Canada and the Canadian Academy of Engineering, and is a Registered Professional Engineer in the Province of Ontario.